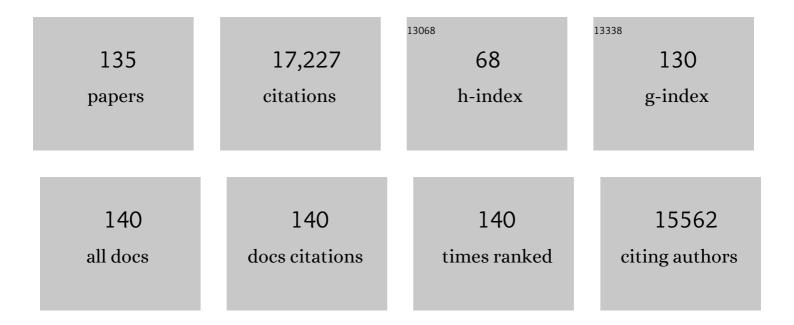
List of Publications by Year in descending order

Source: https://exaly.com/author-pdf/1682459/publications.pdf Version: 2024-02-01



#	Article	IF	CITATIONS
1	Electrochemical Reduction of N <sub>2</sub> under Ambient Conditions for Artificial N <sub>2</sub> Fixation and Renewable Energy Storage Using N <sub>2</sub> /NH <sub>3</sub> Cycle. Advanced Materials, 2017, 29, 1604799.	11.1	969
2	In Situ Coupling of Strung Co <sub>4</sub> N and Intertwined N–C Fibers toward Free-Standing Bifunctional Cathode for Robust, Efficient, and Flexible Zn–Air Batteries. Journal of the American Chemical Society, 2016, 138, 10226-10231.	6.6	839
3	Au Subâ€Nanoclusters on TiO <sub>2</sub> toward Highly Efficient and Selective Electrocatalyst for N <sub>2</sub> Conversion to NH <sub>3</sub> at Ambient Conditions. Advanced Materials, 2017, 29, 1606550.	11.1	785
4	Amorphizing of Au Nanoparticles by CeO <i><sub>x</sub></i> –RGO Hybrid Support towards Highly Efficient Electrocatalyst for N <sub>2</sub> Reduction under Ambient Conditions. Advanced Materials, 2017, 29, 1700001.	11.1	518
5	Anchoring PdCu Amorphous Nanocluster on Graphene for Electrochemical Reduction of N <sub>2</sub> to NH <sub>3</sub> under Ambient Conditions in Aqueous Solution. Advanced Energy Materials, 2018, 8, 1800124.	10.2	454
6	One-Step Seeding Growth of Magnetically Recyclable Au@Co Coreâ^'Shell Nanoparticles: Highly Efficient Catalyst for Hydrolytic Dehydrogenation of Ammonia Borane. Journal of the American Chemical Society, 2010, 132, 5326-5327.	6.6	453
7	Artificial Protection Film on Lithium Metal Anode toward Longâ€Cycleâ€Life Lithium–Oxygen Batteries. Advanced Materials, 2015, 27, 5241-5247.	11.1	439
8	Ironâ€Nanoparticleâ€Catalyzed Hydrolytic Dehydrogenation of Ammonia Borane for Chemical Hydrogen Storage. Angewandte Chemie - International Edition, 2008, 47, 2287-2289.	7.2	433
9	Liquidâ€Phase Chemical Hydrogen Storage: Catalytic Hydrogen Generation under Ambient Conditions. ChemSusChem, 2010, 3, 541-549.	3.6	396
10	Materials Design and System Construction for Conventional and New oncept Supercapacitors. Advanced Science, 2017, 4, 1600382.	5.6	365
11	Noble-metal-free cobalt phosphide modified carbon nitride: An efficient photocatalyst for hydrogen generation. Applied Catalysis B: Environmental, 2017, 200, 477-483.	10.8	364
12	Electrospun materials for lithium and sodium rechargeable batteries: from structure evolution to electrochemical performance. Energy and Environmental Science, 2015, 8, 1660-1681.	15.6	362
13	Reactive Multifunctional Templateâ€Induced Preparation of Feâ€Nâ€Doped Mesoporous Carbon Microspheres Towards Highly Efficient Electrocatalysts for Oxygen Reduction. Advanced Materials, 2016, 28, 7948-7955.	11.1	342
14	Boron- and nitrogen-based chemical hydrogen storage materials. International Journal of Hydrogen Energy, 2009, 34, 2303-2311.	3.8	337
15	An Efficient CoAuPd/C Catalyst for Hydrogen Generation from Formic Acid at Room Temperature. Angewandte Chemie - International Edition, 2013, 52, 4406-4409.	7.2	337
16	Prevention of dendrite growth and volume expansion to give high-performance aprotic bimetallic Li-Na alloy–O2 batteries. Nature Chemistry, 2019, 11, 64-70.	6.6	265
17	Amorphizing of Cu Nanoparticles toward Highly Efficient and Robust Electrocatalyst for CO <sub>2</sub> Reduction to Liquid Fuels with High Faradaic Efficiencies. Advanced Materials, 2018, 30, e1706194.	11.1	242
18	Transformation of Rusty Stainlessâ€Steel Meshes into Stable, Lowâ€Cost, and Binderâ€Free Cathodes for Highâ€Performance Potassiumâ€Ion Batteries. Angewandte Chemie - International Edition, 2017, 56, 7881-7885.	7.2	241

#	Article	IF	CITATIONS
19	Generating Defectâ€Rich Bismuth for Enhancing the Rate of Nitrogen Electroreduction to Ammonia. Angewandte Chemie - International Edition, 2019, 58, 9464-9469.	7.2	226
20	Highly Efficient Photoelectrochemical Water Splitting: Surface Modification of Cobaltâ€Phosphate‣oaded Co <sub>3</sub> O <sub>4</sub> /Fe <sub>2</sub> O <sub>3</sub> p–n Heterojunction Nanorod Arrays. Advanced Functional Materials, 2019, 29, 1801902.	7.8	220
21	Single or Double: Which Is the Altar of Atomic Catalysts for Nitrogen Reduction Reaction?. Small Methods, 2019, 3, 1800291.	4.6	210
22	AuPd–MnO <sub>x</sub> /MOF–Graphene: An Efficient Catalyst for Hydrogen Production from Formic Acid at Room Temperature. Advanced Energy Materials, 2015, 5, 1500107.	10.2	203
23	Room temperature hydrolytic dehydrogenation of ammonia borane catalyzed by Co nanoparticles. Journal of Power Sources, 2010, 195, 1091-1094.	4.0	202
24	High-Energy-Density Flexible Potassium-Ion Battery Based on Patterned Electrodes. Joule, 2018, 2, 736-746.	11.7	199
25	Au@Pd core–shell nanoclusters growing on nitrogen-doped mildly reduced graphene oxide with enhanced catalytic performance for hydrogen generation from formic acid. Journal of Materials Chemistry A, 2013, 1, 12721.	5.2	196
26	Advanced catalysts for sustainable hydrogen generation and storage via hydrogen evolution and carbon dioxide/nitrogen reduction reactions. Progress in Materials Science, 2018, 92, 64-111.	16.0	195
27	Synthesis of Longtime Water/Air-Stable Ni Nanoparticles and Their High Catalytic Activity for Hydrolysis of Ammoniaâ~'Borane for Hydrogen Generation. Inorganic Chemistry, 2009, 48, 7389-7393.	1.9	185
28	Reconstructed Orthorhombic V2O5 Polyhedra for Fast Ion Diffusion in K-Ion Batteries. CheM, 2019, 5, 168-179.	5.8	174
29	Pd/C Synthesized with Citric Acid: An Efficient Catalyst for Hydrogen Generation from Formic Acid/Sodium Formate. Scientific Reports, 2012, 2, 598.	1.6	173
30	Preparation and catalysis of poly(N-vinyl-2-pyrrolidone) (PVP) stabilized nickel catalyst for hydrolytic dehydrogenation of ammonia borane. International Journal of Hydrogen Energy, 2009, 34, 3816-3822.	3.8	170
31	Magnetically Recyclable Fe@Pt Coreâ^'Shell Nanoparticles and Their Use as Electrocatalysts for Ammonia Borane Oxidation: The Role of Crystallinity of the Core. Journal of the American Chemical Society, 2009, 131, 2778-2779.	6.6	170
32	Synthesis of Potassiumâ€Modified Graphitic Carbon Nitride with High Photocatalytic Activity for Hydrogen Evolution. ChemSusChem, 2014, 7, 2654-2658.	3.6	166
33	In situ anchoring of Co9S8 nanoparticles on N and S co-doped porous carbon tube as bifunctional oxygen electrocatalysts. NPG Asia Materials, 2016, 8, e308-e308.	3.8	164
34	Recent Advances toward the Rational Design of Efficient Bifunctional Air Electrodes for Rechargeable Zn–Air Batteries. Small, 2018, 14, e1703843.	5.2	163
35	In Situ Construction of Stable Tissueâ€Directed/Reinforced Bifunctional Separator/Protection Film on Lithium Anode for Lithium–Oxygen Batteries. Advanced Materials, 2017, 29, 1606552.	11.1	162
36	Magnetically recyclable Fe–Ni alloy catalyzed dehydrogenation of ammonia borane in aqueous solution under ambient atmosphere. Journal of Power Sources, 2009, 194, 478-481.	4.0	156

#	Article	IF	CITATIONS
37	Anchoring and Upgrading Ultrafine NiPd on Roomâ€Temperatureâ€Synthesized Bifunctional NH <sub>2</sub> â€Nâ€rGO toward Lowâ€Cost and Highly Efficient Catalysts for Selective Formic Acid Dehydrogenation. Advanced Materials, 2018, 30, e1703038.	11.1	156
38	Reversible Nitrogen Fixation Based on a Rechargeable Lithium-Nitrogen Battery for Energy Storage. CheM, 2017, 2, 525-532.	5.8	146
39	Hollow Ni–SiO2 nanosphere-catalyzed hydrolytic dehydrogenation of ammonia borane for chemical hydrogen storage. Journal of Power Sources, 2009, 191, 209-216.	4.0	138
40	Rapid and energy-efficient synthesis of a graphene–CuCo hybrid as a high performance catalyst. Journal of Materials Chemistry, 2012, 22, 10990.	6.7	136
41	Non-noble metals applied to solar water splitting. Energy and Environmental Science, 2018, 11, 3128-3156.	15.6	134
42	Decorating Waste Cloth via Industrial Wastewater for Tubeâ€Type Flexible and Wearable Sodiumâ€Ion Batteries. Advanced Materials, 2017, 29, 1603719.	11.1	131
43	Enhancing photocatalytic activity of disorder-engineered C/TiO <sub>2</sub> and TiO <sub>2</sub> nanoparticles. Journal of Materials Chemistry A, 2014, 2, 7439-7445.	5.2	130
44	Engineering Ultrathin C <sub>3</sub> N <sub>4</sub> Quantum Dots on Graphene as a Metal-Free Water Reduction Electrocatalyst. ACS Catalysis, 2018, 8, 3965-3970.	5.5	130
45	Boosting Production of HCOOH from CO <sub>2</sub> Electroreduction via Bi/CeO <sub><i>x</i></sub> . Angewandte Chemie - International Edition, 2021, 60, 8798-8802.	7.2	130
46	In Situ Coupling FeM (M = Ni, Co) with Nitrogenâ€Đoped Porous Carbon toward Highly Efficient Trifunctional Electrocatalyst for Overall Water Splitting and Rechargeable Zn–Air Battery. Advanced Sustainable Systems, 2017, 1, 1700020.	2.7	122
47	Ag0.1-Pd0.9/rGO: an efficient catalyst for hydrogen generation from formic acid/sodium formate. Journal of Materials Chemistry A, 2013, 1, 12188.	5.2	121
48	Hydrogen generation from formic acid decomposition at room temperature using a NiAuPd alloy nanocatalyst. International Journal of Hydrogen Energy, 2014, 39, 4850-4856.	3.8	121
49	Flexible and Foldable Li–O <sub>2</sub> Battery Based on Paperâ€Ink Cathode. Advanced Materials, 2015, 27, 8095-8101.	11.1	117
50	Synthesis of g-C3N4 with heating acetic acid treated melamine and its photocatalytic activity for hydrogen evolution. Applied Surface Science, 2015, 354, 196-200.	3.1	117
51	Highly efficient hydrogen generation from hydrous hydrazine over amorphous Ni0.9Pt0.1/Ce2O3 nanocatalyst at room temperature. Journal of Materials Chemistry A, 2013, 1, 14957.	5.2	116
52	Carbon quantum dot sensitized integrated Fe <sub>2</sub> O <sub>3</sub> @g-C <sub>3</sub> N <sub>4</sub> core–shell nanoarray photoanode towards highly efficient water oxidation. Journal of Materials Chemistry A, 2018, 6, 9839-9845.	5.2	110
53	Recent advances in metal–nitrogen–carbon catalysts for electrochemical water splitting. Materials Chemistry Frontiers, 2017, 1, 2155-2173.	3.2	109
54	Bloodâ€Capillaryâ€Inspired, Freeâ€Standing, Flexible, and Lowâ€Cost Superâ€Hydrophobic Nâ€CNTs@SS Catho for Highâ€Capacity, Highâ€Rate, and Stable Liâ€Air Batteries. Advanced Energy Materials, 2018, 8, 1702242.	odes 10.2	108

#	Article	IF	CITATIONS
55	Ag <sub>2</sub> O modified g-C <sub>3</sub> N <sub>4</sub> for highly efficient photocatalytic hydrogen generation under visible light irradiation. Journal of Materials Chemistry A, 2015, 3, 15710-15714.	5.2	103
56	Facile synthesis of nitrogen-doped graphene supported AuPd–CeO2 nanocomposites with high-performance for hydrogen generation from formic acid at room temperature. Nanoscale, 2014, 6, 3073.	2.8	99
57	Iron-chelated hydrogel-derived bifunctional oxygen electrocatalyst for high-performance rechargeable Zn–air batteries. Nano Research, 2017, 10, 4436-4447.	5.8	98
58	Simultaneous Achieving of High Faradaic Efficiency and CO Partial Current Density for CO <sub>2</sub> Reduction via Robust, Nobleâ€Metalâ€Free Zn Nanosheets with Favorable Adsorption Energy. Advanced Energy Materials, 2019, 9, 1900276.	10.2	95
59	A Simple and Effective Principle for a Rational Design of Heterogeneous Catalysts for Dehydrogenation of Formic Acid. Advanced Materials, 2019, 31, e1806781.	11.1	95
60	Facile synthesis of AgAuPd/graphene with high performance for hydrogen generation from formic acid. Journal of Materials Chemistry A, 2015, 3, 14535-14538.	5.2	94
61	One-step synthesis of Cu@FeNi core–shell nanoparticles: Highly active catalyst for hydrolytic dehydrogenation of ammonia borane. International Journal of Hydrogen Energy, 2012, 37, 10229-10235.	3.8	90
62	DNA-directed growth of ultrafine CoAuPd nanoparticles on graphene as efficient catalysts for formic acid dehydrogenation. Chemical Communications, 2014, 50, 2732.	2.2	87
63	Tailoring Oxygen Vacancies of BiVO <sub>4</sub> toward Highly Efficient Nobleâ€Metalâ€Free Electrocatalyst for Artificial N <sub>2</sub> Fixation under Ambient Conditions. Small Methods, 2019, 3, 1800333.	4.6	84
64	Noble-metal-free NiFeMo nanocatalyst for hydrogen generation from the decomposition of hydrous hydrazine. Journal of Materials Chemistry A, 2015, 3, 121-124.	5.2	80
65	An Illuminationâ€Assisted Flexible Selfâ€Powered Energy System Based on a Li–O <sub>2</sub> Battery. Angewandte Chemie - International Edition, 2019, 58, 16411-16415.	7.2	78
66	Co–SiO2 nanosphere-catalyzed hydrolytic dehydrogenation of ammonia borane for chemical hydrogen storage. Journal of Power Sources, 2010, 195, 8209-8214.	4.0	76
67	Amorphous nickel pyrophosphate modified graphitic carbon nitride: an efficient photocatalyst for hydrogen generation from water splitting. Applied Catalysis B: Environmental, 2018, 231, 43-50.	10.8	75
68	Efficient CO <sub>2</sub> Reduction to HCOOH with High Selectivity and Energy Efficiency over Bi/rGO Catalyst. Small Methods, 2020, 4, 1900846.	4.6	70
69	A new fuel cell using aqueous ammonia-borane as the fuel. Journal of Power Sources, 2007, 168, 167-171.	4.0	69
70	Efficient visible-light-driven hydrogen generation from water splitting catalyzed by highly stable CdS@Mo <sub>2</sub> C–C core–shell nanorods. Journal of Materials Chemistry A, 2017, 5, 15862-15868.	5.2	67
71	Green and Facile Fabrication of MWNTs@Sb <sub>2</sub> S <sub>3</sub> @PPy Coaxial Nanocables for Highâ€Performance Naâ€lon Batteries. Particle and Particle Systems Characterization, 2016, 33, 493-499.	1.2	66
72	A Waterâ€∤Fireproof Flexible Lithium–Oxygen Battery Achieved by Synergy of Novel Architecture and Multifunctional Separator. Advanced Materials, 2018, 30, 1703791.	11.1	65

#	Article	IF	CITATIONS
73	Integrating 3D Flower-Like Hierarchical Cu <sub>2</sub> NiSnS <sub>4</sub> with Reduced Graphene Oxide as Advanced Anode Materials for Na-Ion Batteries. ACS Applied Materials & Interfaces, 2016, 8, 9178-9184.	4.0	64
74	In Situ CVD Derived Co–N–C Composite as Highly Efficient Cathode for Flexible Li–O <sub>2</sub> Batteries. Small, 2018, 14, e1800590.	5.2	64
75	Suppressing Sodium Dendrites by Multifunctional Polyvinylidene Fluoride (PVDF) Interlayers with Nonthrough Pores and High Flux/Affinity of Sodium Ions toward Long Cycle Life Sodium Oxygenâ€Batteries. Advanced Functional Materials, 2018, 28, 1703931.	7.8	54
76	Composition-tunable synthesis of "clean―syngas via a one-step synthesis of metal-free pyridinic-N-enriched self-supported CNTs: the synergy of electrocatalyst pyrolysis temperature and potential. Green Chemistry, 2017, 19, 4284-4288.	4.6	53
77	Recent Progresses and Prospects of Cathode Materials for Non-aqueous Potassium-Ion Batteries. Electrochemical Energy Reviews, 2018, 1, 548-566.	13.1	48
78	Nitrogen Reduction Reaction. Small Methods, 2019, 3, 1900070.	4.6	48
79	Generating Defectâ€Rich Bismuth for Enhancing the Rate of Nitrogen Electroreduction to Ammonia. Angewandte Chemie, 2019, 131, 9564-9569.	1.6	47
80	High catalytic kinetic performance of amorphous CoPt NPs induced on CeO for H2 generation from hydrous hydrazine. International Journal of Hydrogen Energy, 2014, 39, 3755-3761.	3.8	46
81	Transformation of Rusty Stainlessâ€Steel Meshes into Stable, Lowâ€Cost, and Binderâ€Free Cathodes for Highâ€Performance Potassiumâ€Ion Batteries. Angewandte Chemie, 2017, 129, 7989-7993.	1.6	46
82	External Electric Field Catalyzed N <sub>2</sub> O Decomposition on Mn-Embedded Graphene. Journal of Physical Chemistry C, 2012, 116, 20342-20348.	1.5	44
83	Complete Dehydrogenation of N <sub>2</sub> H <sub>4</sub> BH <sub>3</sub> over Nobleâ€Metalâ€Free Ni <sub>0.5</sub> Fe <sub>0.5</sub> –CeO <i><sub>x</sub></i> /MILâ€101 with High Activity and 100% H <sub>2</sub> Selectivity. Advanced Energy Materials, 2018, 8, 1800625.	10.2	44
84	Facile Synthesis of an Ag <sub>2</sub> O–ZnO Nanohybrid and Its High Photocatalytic Activity. ChemPlusChem, 2012, 77, 931-935.	1.3	43
85	P3-type K <sub>0.33</sub> Co <sub>0.53</sub> Mn <sub>0.47</sub> O <sub>2</sub> ·0.39H <sub>2</sub> O: a novel bifunctional electrode for Na-ion batteries. Materials Horizons, 2017, 4, 1122-1127.	6.4	41
86	Hybrid solid electrolyte enabled dendrite-free Li anodes for high-performance quasi-solid-state lithium-oxygen batteries. National Science Review, 2021, 8, nwaa150.	4.6	41
87	Integrated Cu <sub>3</sub> N porous nanowire array electrode for high-performance supercapacitors. Journal of Materials Chemistry A, 2017, 5, 18972-18976.	5.2	40
88	A Low-Volatile and Durable Deep Eutectic Electrolyte for High-Performance Lithium–Oxygen Battery. Journal of the American Chemical Society, 2022, 144, 5827-5833.	6.6	39
89	Nobleâ€Metalâ€Free Niâ€MoO <i><sub>x</sub></i> Nanoparticles Supported on BN as a Highly Efficient Catalyst toward Complete Decomposition of Hydrazine Borane. Small Methods, 2018, 2, 1800250.	4.6	38
90	High spin polarization ultrafine Rh nanoparticles on CNT for efficient electrochemical N2 fixation to ammonia. Applied Catalysis B: Environmental, 2021, 298, 120592.	10.8	38

#	Article	IF	CITATIONS
91	A high performance anion exchange membrane-type ammonia borane fuel cell. Journal of Power Sources, 2008, 182, 515-519.	4.0	37
92	Ni/La2O3 catalyst containing low content platinum–rhodium for the dehydrogenation of N2H4·H2O at room temperature. Journal of Power Sources, 2014, 262, 386-390.	4.0	36
93	Electrochemical oxidation of ammonia borane on gold electrode. International Journal of Hydrogen Energy, 2009, 34, 174-179.	3.8	35
94	Facile preparation of N-doped carbon nanofiber aerogels from bacterial cellulose as an efficient oxygen reduction reaction electrocatalyst. Chinese Journal of Catalysis, 2014, 35, 877-883.	6.9	35
95	Growth of Ruâ€Modified Co <sub>3</sub> O <sub>4</sub> Nanosheets on Carbon Textiles toward Flexible and Efficient Cathodes for Flexible Li–O <sub>2</sub> Batteries. Particle and Particle Systems Characterization, 2016, 33, 500-505.	1.2	33
96	Synthesis of porous and metallic CoB nanosheets towards a highly efficient electrocatalyst for rechargeable Na–O <sub>2</sub> batteries. Energy and Environmental Science, 2018, 11, 2833-2838.	15.6	33
97	Regulating Fe <sub>2</sub> (MoO <sub>4</sub> ) <sub>3</sub> by Au Nanoparticles for Efficient N <sub>2</sub> Electroreduction under Ambient Conditions. Advanced Energy Materials, 2021, 11, 2003701.	10.2	31
98	Cu4 Cluster Doped Monolayer MoS2 for CO Oxidation. Scientific Reports, 2015, 5, 11230.	1.6	30
99	Soluble and Perfluorinated Polyelectrolyte for Safe and Highâ€Performance Liâ °O <sub>2</sub> Batteries. Angewandte Chemie - International Edition, 2022, 61, e202116635.	7.2	28
100	Photoinduced decoration of NiO nanosheets/Ni foam with Pd nanoparticles towards a carbon-free and self-standing cathode for a lithium–oxygen battery with a low overpotential and long cycle life. Materials Horizons, 2018, 5, 298-302.	6.4	27
101	Crystal Structure and Carbon Vacancy Hardening of (W0.5Al0.5)C1â^'x Prepared by a Solid-State Reaction. ChemPhysChem, 2005, 6, 2099-2103.	1.0	26
102	Tri-metallic AuPdIr nanoalloy towards efficient hydrogen generation from formic acid. Applied Catalysis B: Environmental, 2022, 309, 121228.	10.8	25
103	Single Layer of Polymeric Metal–Phthalocyanine: Promising Substrate to Realize Single Pt Atom Catalyst with Uniform Distribution. Journal of Physical Chemistry C, 2014, 118, 2122-2128.	1.5	24
104	Hydrogenâ€Bondâ€Assisted Solution Discharge in Aprotic Li–O <sub>2</sub> Batteries. Advanced Materials, 2022, 34, e2110416.	11.1	24
105	Synthesis, crystal structure, and density of (W1â^'xAlx)C. Journal of Solid State Chemistry, 2004, 177, 2265-2270.	1.4	23
106	Oleylamine-stabilized Cu 0.9 Ni 0.1 nanoparticles as efficient catalyst for ammonia borane dehydrogenation. International Journal of Hydrogen Energy, 2017, 42, 25251-25257.	3.8	22
107	P3-type K <sub>0.32</sub> Fe <sub>0.35</sub> Mn <sub>0.65</sub> O <sub>2</sub> ·0.39H <sub>2</sub> O: a promising cathode for Na-ion full batteries. Journal of Materials Chemistry A, 2018, 6, 13075-13081.	5.2	22
108	Co/La-Doped NiO Hollow Nanocubes Wrapped with Reduced Graphene Oxide for Lithium Storage. ACS Applied Nano Materials, 2021, 4, 2910-2920.	2.4	19

#	Article	IF	CITATIONS
109	Enabling Pyrochlore-Type Oxides as Highly Efficient Electrocatalysts for High-Capacity and Stable Na–O <sub>2</sub> Batteries: The Synergy of Electronic Structure and Morphology. ACS Catalysis, 2017, 7, 7688-7694.	5.5	18
110	Processing, microstructure and mechanical properties of WAI bulk alloy obtained by mechanical alloying and hot-pressing. Scripta Materialia, 2004, 51, 993-997.	2.6	16
111	Synthesis, reactive mechanism and thermal stability of W1â^'xAlxC (x=0.33, 0.5, 0.75, 0.86) nanocrystalline. Materials Research Bulletin, 2004, 39, 707-713.	2.7	16
112	Synthesis and thermal stability of Al75W25 alloy obtained by mechanically alloying. Journal of Alloys and Compounds, 2005, 393, 248-251.	2.8	16
113	Self-protective cobalt nanocatalyst for long-time recycle application on hydrogen generation by its free metal-ion conversion. Journal of Power Sources, 2013, 243, 431-435.	4.0	16
114	Non-noble-metal bismuth nanoparticle-decorated bismuth vanadate nanoarray photoanode for efficient water splitting. Materials Chemistry Frontiers, 2018, 2, 1799-1804.	3.2	13
115	Creation of a rigid host framework with optimum crystal structure and interface for zero-strain K-ion storage. Energy and Environmental Science, 2022, 15, 1529-1535.	15.6	12
116	Supported ultrafine NiPt–MoO <sub><i>x</i></sub> nanocomposites as highly efficient catalysts for complete dehydrogenation of hydrazine borane. Journal of Materials Chemistry A, 2021, 9, 26704-26708.	5.2	11
117	Three Birds with One Stone: An Integrated Cathode–Electrolyte Structure for Highâ€Performance Solidâ€ <del>S</del> tate Lithium–Oxygen Batteries. Small, 2022, 18, e2107833.	5.2	11
118	High-pressure sintering study of a novel hard material (W0.5Al0.5)C0.5 without binder metal. International Journal of Refractory Metals and Hard Materials, 2007, 25, 62-66.	1.7	10
119	Hybrid Film from Nickel Oxide and Oxygenated Carbon Nanotube as Flexible Electrodes for Pseudocapacitors. ChemNanoMat, 2016, 2, 698-703.	1.5	10
120	Crystallization of mechanically alloyed amorphous W–Mg alloy under high pressure. Solid State Communications, 2004, 129, 147-150.	0.9	9
121	Synthesis and high-pressure sintering of (W0.5Al0.5)C. Materials Research Bulletin, 2005, 40, 701-707.	2.7	9
122	Preparation of W–Al–Mo ternary alloys by mechanical alloying. Journal of Alloys and Compounds, 2007, 430, 77-80.	2.8	9
123	Efficient nitrate-to-ammonia transformation through a direct eight-electron reduction. Science China Chemistry, 2020, 63, 1737-1739.	4.2	8
124	Synthesis and characterization of (W0.8Al0.2)C0.8 deduction solid solution. Materials Science and Engineering B: Solid-State Materials for Advanced Technology, 2005, 117, 321-324.	1.7	5
125	Crystallization and characterization of substoichiometric compound (W0.5Al0.5)C0.5 obtained by solid-state reaction. Metallurgical and Materials Transactions A: Physical Metallurgy and Materials Science, 2006, 37, 1692-1695.	1.1	5
126	Synthesis, Microstructure and Mechanical Properties of Al40W60 Bulk Alloy Obtained by Mechanical Alloying and Hot-Pressing. Advanced Engineering Materials, 2005, 7, 256-260.	1.6	4

#	Article	IF	CITATIONS
127	Bulk ultrafine binderless (W0.4Al0.6)C prepared by high pressure sintering. Journal of Alloys and Compounds, 2008, 453, 382-385.	2.8	4
128	Soluble and Perfluorinated Polyelectrolyte for Safe and Highâ€Performance Liâ^'O <sub>2</sub> Batteries. Angewandte Chemie, 2022, 134, .	1.6	4
129	Synthesis, structure and reactive mechanism of intermetallic W4Mg. Journal of Alloys and Compounds, 2003, 354, 236-238.	2.8	3
130	Boosting Production of HCOOH from CO 2 Electroreduction via Bi/CeO x. Angewandte Chemie, 2021, 133, 8880-8884.	1.6	3
131	Synthesis, structure and reactive mechanism of intermetallic W3Mg. Intermetallics, 2003, 11, 893-896.	1.8	2
132	Processing, Microstructure and Mechanical Properties of in Situ Al-based Metal Matrix Composite Reinforced with 22 wt%WAl12 Particles. Advanced Engineering Materials, 2006, 8, 740-743.	1.6	2
133	Preparation and characterization of a novel solid solution of aluminum in tungsten carbide by mechanically activated high-temperature reaction. Journal of Materials Research, 2006, 21, 1700-1703.	1.2	2
134	Electron polarization induced by alloying changes mechanism of NH3 synthesis from NO3â^' electroreduction. Chem Catalysis, 2021, 1, 970-972.	2.9	2
135	Synthesis and Characterization of the Off-Stoichiometric Compound (W0.8Al0.2)C0.7. Advanced Engineering Materials, 2005, 7, 130-133.	1.6	1